Journal of Exploratory Research in Pharmacology **2024** vol. 9(4) | 238–251
DOI: 10.14218/JERP.2024.00014

Original Article

Dihydroartemisinin Inhibits T Cell Activation in People Living with HIV with Incomplete Immune Reconstitution *In Vitro*

Yang Zhang[1,2,3#], Jiahao Ji[1#], Xiaodong Dou[4], Rui Wang[1,2], Hao Wu[1,2,3], Zhen Li[1,2*] and Tong Zhang[1,2,3*]

[1]Center for Infectious Diseases, Beijing Youan Hospital, Capital Medical University, Beijing, China; [2]Beijing Key Laboratory of HIV/AIDS Research, Beijing, China; [3]Beijing Institute of Sexually Transmitted Disease Prevention and Control, Beijing, China; [4]State Key Laboratory of Natural and Biomimetic Drugs, School of Pharmaceutical Science, Peking University, Beijing, China

Received: March 27, 2024 | **Revised:** October 09, 2024 | **Accepted:** October 23, 2024 | **Published online:** December 30, 2024

Abstract

Background and objectives: Incomplete immune reconstitution is characterized by chronic immune activation and systemic inflammation, which are not fully reversed by antiretroviral therapy. Dihydroartemisinin (DHA) has demonstrated anti-inflammatory and immunosuppressive properties, which may benefit individuals with incomplete immune reconstitution. This study aimed to investigate the biological mechanisms underlying incomplete immune reconstitution and evaluate the therapeutic potential of DHA in modulating immune activation in immunological non-responders (INRs). This study aimed to investigate the biological mechanisms underlying incomplete immune reconstitution and evaluate the therapeutic potential of DHA in modulating immune activation in immunological non-responders (INRs).

Methods: RNA sequencing data (GSE106792) was retrieved from the Gene Expression Omnibus database. R software and Bioconductor packages were used to identify differentially expressed genes (DEGs) among INRs, immune responders (IRs), and healthy controls (HCs). Gene Ontology and Kyoto Encyclopedia of Genes and Genomes enrichment analyses, along with protein-protein interaction (PPI) network construction, were performed. Potential DHA-binding proteins were predicted using the STITCH server and molecular docking studies. Validation experiments were conducted on peripheral blood mononuclear cells from 18 INRs. Cells were treated with varying concentrations of DHA, and $CD4^+$ and $CD8^+$ T cell activation markers (CD38 and HLA-DR) were measured via flow cytometry.

Results: Enrichment and PPI network analysis identified 119, 56, and 189 DEGs in the INR vs. HC, INR vs. IR, and IR vs. HC comparisons, respectively. Enrichment and PPI analyses showed that DEGs were mainly involved in immune response pathways. DHA was predicted to interact with multiple target proteins, indicating anti-inflammatory effects. *In vitro*, DHA significantly reduced the frequency of $CD38^-$ HLA-DR^+ $CD4^+$ T cells and $CD38^+$ HLA-DR^+ $CD8^+$ T cells at 1,000 μM and 500 μM compared to the control.

Conclusions: This study provides insights into the biological mechanisms underlying incomplete immune reconstitution and supports DHA's potential as a therapeutic agent. DHA effectively inhibits T cell activation in INRs, presenting a novel and promising treatment strategy.

Keywords: Dihydroartemisinin; DHA; HIV; AIDS; Immunological non-responders; $CD4^+$ T-cell; Immune activation.

***Correspondence to:** Zhen Li, Center for Infectious Diseases, Beijing YouAn Hospital, Capital Medical University, 8 Xitoutiao, Youanmenwai, Fengtai District, Beijing 100069, China. ORCID: https://orcid.org/0000-0003-0298-1677. Tel: +86-10-83997644, Fax: +86-10-83997644, E-mail: lizhen_youan@ccmu.edu.cn; Tong Zhang, Center for Infectious Diseases, Beijing Youan Hospital, Capital Medical University, 8 Xitoutiao, Youanmenwai, Fengtai District, Beijing, 100069. ORCID: https://orcid.org/0000-0003-2534-4785. Tel: +10-8399764, Fax: +86-10-83997644, China. E-mail: zt_doc@ccmu.edu.cn

[#]These authors contributed equally to this work.

How to cite this article: Zhang Y, Ji J, Dou X, Wang R, Wu H, Li Z, *et al*. Dihydroartemisinin Inhibits T Cell Activation in People Living with HIV with Incomplete Immune Reconstitution *In Vitro*. *J Explor Res Pharmacol* 2024;9(4):238–251. doi: 10.14218/JERP.2024.00014.

Introduction

Despite effective antiretroviral therapy (ART), people living with HIV (PLWH), particularly those with incomplete $CD4^+$ T-cell recovery on ART, remain at higher risk for age-related morbidities.[1–3] Although CD4 depletion is a hallmark of HIV disease progression, immune activation and inflammation also play critical roles in HIV pathogenesis, as well as in the occurrence of serious non-AIDS events in immunological non-responders (INRs).[4–8] Thus, interventions aimed at reducing inflammation and immune activation may provide a clearer understanding of the underlying

pathogenesis and offer potential therapeutic benefits. Since 2001, scientists have attempted to treat INRs with medications such as prednisone,[9] hydroxychloroquine,[10] and other non-specific candidates, including atorvastatin,[11] valganciclovir,[12] rifaximin,[13] and maraviroc.[14] However, our recent systematic review and meta-analysis showed that while some of these candidates can reduce immune activation or chronic inflammation, they rarely have the desired effect of directly recovering $CD4^+$ T-cell counts.[15] Therefore, an effective, safe, inexpensive, and convenient intervention that promotes $CD4^+$ T-cell recovery would be highly beneficial. One potential therapeutic target for such an intervention is inflammation and immune activation.

Plants continue to be a vital source of new medicines and chemical entities. Artemisinin and its analogs, such as dihydroartemisinin (DHA), have been used for decades in malaria treatment.[16] DHA has demonstrated numerous beneficial immunomodulatory and anti-inflammatory properties in animal models of lupus arthritis,[17,18] inflammatory bowel disease,[19] and renal fibrosis,[20] conditions characterized by high levels of inflammation and immune activation. Moreover, DHA is a once-daily oral treatment with an excellent long-term safety profile and low cost.[21–23] Therefore, we hypothesized that DHA might be an ideal candidate to reduce immune activation and inflammation, thereby promoting $CD4^+$ T-cell recovery in INRs.

The Gene Expression Omnibus (GEO; http://www.ncbi.nlm.nih.gov/geo/) database has greatly enhanced our understanding of immune activation and inflammation in HIV disease pathogenesis. Fortunately, efficient integrated bioinformatics and chemical informatics methods have been developed for large-scale, cross-platform high-throughput data analysis. In this study, we identified differentially expressed genes (DEGs) from microarray and RNA-seq data. Gene Ontology (GO) function and Kyoto Encyclopedia of Genes and Genomes (KEGG) pathway enrichment analysis, as well as protein-protein interaction (PPI) network analysis of DEGs, were performed. The potential binding proteins of DHA were then predicted through molecular docking. To further confirm the pharmacological effects of DHA, we cultured T cells from INRs under different concentrations of DHA *in vitro*.

Materials and methods

Study approval

Study materials were developed in accordance with the Declaration of Helsinki, along with ethical norms, guidelines, and HIV-related laws and regulations in China. The study was approved by the Ethics Committee of Beijing Youan Hospital, Capital Medical University (No. 2020147).

Data source

The original dataset of gene expression profiles, including immune responders (IRs), INR, and healthy controls (HCs), was downloaded from NCBI's GEO database. The accession number was GSE106792, based on GPL10558 (Illumina HumanHT-12 V4.0 expression bead chip, Illumina Inc, San Diego, CA, USA).[24] The dataset GSE106792 consists of RNA sequencing data from 36 samples: 12 HCs, 12 immune non-responders, and 12 IRs, all derived from $CD4^+$ T cells.

Data normalization and differential gene expression analysis

The robust multi-array average approach, including quantile normalization and log2 transformation, was performed for background correction and normalization to reduce variability. The gene probes in the expression profiles were annotated through the GPL10558 platform, and duplicate gene probes were combined, retaining the higher values. The Limma R package (version 3.44.3) was subsequently employed to identify DEGs,[25] with patient status set as an independent variable while cell subset was not considered as an independent or dependent variable. Absolute $\log_2$FC greater than 1.0 and adjusted *P*-value, based on the Benjamini & Hochberg procedure, less than 0.05 were selected as threshold values. Heatmaps were generated in the pheatmap R package (version 1.0.12) with z-score normalization within each row (gene).

Go and KEGG enrichment analysis

GO and KEGG enrichment analyses were performed using the clusterProfiler R Package (version 3.16.1) and the Database for Annotation,[26] Visualization, and Integrated Discovery (https://david.ncifcrf.gov/).[27] The enrichment analyses, including biological process (BP), cellular component (CC), molecular function (MF), and KEGG pathway, were conducted to investigate the DEGs at the functional level. *P*-value < 0.05 and gene counts ≥ 2 were set as the cutoff criteria.

PPI network construction

The Search Tool for the Retrieval of Interacting Genes (Version 10.5, https://string-db.org) database and Cytoscape software (Version 3.7.2) were employed to construct and visualize the PPI network of the identified DEGs.[28,29] The MCODE module of Cytoscape was used for clustering sub-networks. MCODE scores greater than three and node counts greater than four were applied to screen for the most critical sub-networks in the PPI network.

Chemical association networks

The STITCH (Version 5.0) online server was used to predict the potential target proteins of DHA, and proteins with scores above 0.7 were selected as the threshold value.[30] Meanwhile, an enrichment analysis of the protein-protein interaction network was performed.

Molecular docking

The chemical structure of DHA was processed using the *LigPrep* module in Schrödinger 10.2 software (Schrödinger, LLC, NY, USA).[31] The *Epik* module in Schrödinger was used to generate ionized states and tautomers/stereoisomers at pH = 7.0 ± 2.0.[32] The original chiralities were preserved, and the maximum number of stereoisomers was set to 32, with one low-energy ring conformation generated. The OPLS3 force field was used to perform energy minimization.

The crystallographic structures of the protein complexes were retrieved from the RCSB Protein Data Bank (PDB) and prepared using the Protein Preparation Wizard module in Schrödinger 10.2 software. Proteins were assigned bond orders, hydrogens were added, protonation was performed, crystallographic water molecules were removed, and restrained minimization was carried out until the root-mean-square deviation was lower than 0.3 Å based on the OPLS3 force field.

For each selected crystal structure, DHA was docked into the original ligand-binding site, which had dimensions of 10 Å × 10 Å × 10 Å, using the Glide module in Schrödinger 10.2 software.[33,34] The extra precision option was selected, and all other parameters for Glide were kept at their default values.

ADMET properties prediction of DHA

Animal studies investigating the anti-inflammatory effects of DHA have been published; however, pharmacokinetic data on DHA from clinical trials is still lacking. Therefore, it is necessary to predict the ADMET properties of DHA using the ADMET predictive module of Pipeline Pilot (Version 8.5), which includes aqueous solubility, blood-brain barrier (BBB), cytochrome P450 2D6 binding (CYP2D6), human hepatotoxicity, human intestinal absorption, plasma protein binding (PPB), lipid-water distribution coefficient, and polar surface area. The methods of gradual screening ADMET are as follows: Aqueous solubility: 0 = extremely low; 1 = very low; 2 = low; 3 = good; 4 = optimal; 5 = very soluble. BBB: 0 = very high; 1 = high; 2 = medium; 3 = low; 4 = undefined, the molecule is outside the confidence range of the LogBB regression model). CYP2D6: TRUE = an inhibitor; FALSE = a non-inhibitor. Human hepatotoxicity: TRUE = the compound predicted hepatotoxicity; FALSE = the compound predicted non-hepatotoxicity. Human intestinal absorption: 0 = good; 1 = moderate; 2 = poor; 3 = very poor. PPB: TRUE = compound predicted strong binding (>90%); FALSE = compound predicted weak or no binding (<90%).

DHA validation experiments in vitro

Study subjects

In this study, INRs were defined as HIV-infected patients who had been on ART for more than two years, with plasma viral load completely controlled (plasma HIV RNA levels < 40 copies/mL), and $CD4^+$ T cell counts < 350 cells/μL.[4] We enrolled INRs (n = 18), who were treated with Tenofovir + Lamivudine + Efavirenz for 96 weeks. All the patients were male. The average age was 38.4 ± 7.6 years, and the average $CD4^+$ T cell count was 280.7 ± 53.7 cells/μL. All participants provided written informed consent. Peripheral blood mononuclear cells (PBMCs) were separated from venous blood and used for research. This study was approved by the Beijing YouAn Hospital Research Ethics Committee.

Cell culture

PBMCs were freshly separated and seeded in a 48-well plate at a concentration of 1×10^6 cells/mL. Cells were stimulated with PHA (5 μg/mL) and simultaneously treated with different doses of DHA (1,000 μM, 500 μM, 100 μM, and 0 μM). After 48 h of culture, cells were harvested and used for flow cytometry analysis.

Flow cytometry

Cells were washed with 1% bovine serum albumin in PBS and then incubated with the cell viability marker fixable viability stain 510 (BD Biosciences, San Jose, CA) and labeled with specific surface antibodies for CD3 (HIT3a), CD4 (OKT4), CD8 (SK1), CD38 (HIT2), and HLA-DR (L243). Flow cytometry was performed using a FACScan flow cytometer. Data were analyzed using FlowJo software (Version V10.6.2; Tree Star Inc., Ashland, OR, USA). Cells were sequentially gated on lymphocytes, live cells, single cells, and $CD3^+$ T cells. Then, CD38 and HLA-DR expression on $CD4^+$ T cells and $CD8^+$ T cells were analyzed separately. For further details, see the Supplementary Method for cell proliferation detection.

Statistical analysis

CD38 and HLA-DR expression on $CD4^+$ and $CD8^+$ T cells were presented as percentages and compared across groups using one-way ANOVA. Post-hoc comparisons between groups were conducted using Tukey's test to identify significant differences. All statistical analyses were performed using SPSS 21.0. A *P*-value of < 0.05 was considered statistically significant.

Results

Identification of DEGs among the IR, INR, and HC groups

After data normalization (Fig. S1), as shown in Figure 1a, 119 DEGs were identified in the INR vs. HC groups, 56 DEGs in the INR vs. IR groups, and 189 DEGs in the IR vs. HC groups. Among the identified DEGs, 30, 22, and 22 genes were downregulated, while 89, 34, and 167 genes were upregulated in the INR vs. HC groups, INR vs. IR groups, and IR vs. HC groups, respectively (Figs. S2–S4).

Functional enrichment analysis

To investigate the enrichment and pathway distribution of the aforementioned DEGs, GO and KEGG enrichment analyses were performed using the clusterProfiler R package and the database for Annotation, Visualization, and Integrated Discovery. In the INR vs. HC groups, GO analysis enriched 119 DEGs into 375 BPs, 8 CCs, and 21 MFs (Fig. 1b). In the BP term, the DEGs were primarily involved in leukocyte migration, cell chemotaxis, positive regulation of cell activation, regulation of response to biotic stimulus, negative regulation of phosphorylation, leukocyte chemotaxis, regulation of the innate immune response, response to bacterial molecules, positive regulation of leukocyte activation, and positive regulation of defense response (Fig. 1b).In the CC term, the DEGs were mainly enriched in the secretory granule lumen, cytoplasmic vesicle lumen, vesicle lumen, leading edge membrane, mast cell granule, tertiary granule membrane, specific granule membrane, and ruffle membrane (Fig. 1b).In the MF term, the DEGs were primarily related to cytokine receptor activity, immune receptor activity, carbohydrate binding, cytokine binding, serine-type peptidase activity, hydrolase activity acting on acid-phosphorus-nitrogen bonds, serine hydrolase activity, non-membrane spanning protein tyrosine kinase activity, antioxidant activity, protein tyrosine kinase binding, phospholipase activity, RAGE receptor binding, C-C chemokine receptor activity, C-C chemokine binding, and G protein-coupled chemoattractant receptor activity (Fig. 1b).KEGG pathway analysis revealed that the DEGs were mainly associated with cytokine-cytokine receptor interaction, chemokine signaling pathway, and HIF-1 signaling pathway (Fig. 1b).

In the INR vs. IR groups, GO analysis enriched 56 DEGs into 119 BPs, 14 CCs, and three MFs terms (Fig. 1c). In the BP term, the DEGs were mainly involved in positive regulation of GTPase activity, regulation of translation, regulation of cellular amide metabolic processes, regulation of lymphocyte activation, modulation of processes of other organisms involved in symbiotic interactions, smoothened signaling pathway, viral transcription, viral gene expression, translational initiation, nuclear-transcribed mRNA catabolic processes, cellular response to transforming growth factor beta stimulus, and response to transforming growth factor beta (Fig. 1c). In the CC term, the DEGs were primarily enriched in the transport vesicle membrane, intrinsic component of organelle membrane, transport vesicle, nuclear envelope, endosome membrane, recycling endosome membrane, melanosome, pigment granule, inner mitochondrial membrane protein complex, early endosome membrane, RNA polymerase II transcription regulator complex, anchored component of the membrane, recycling endosome, and coated vesicle membrane (Fig. 1c). In the MF term, the

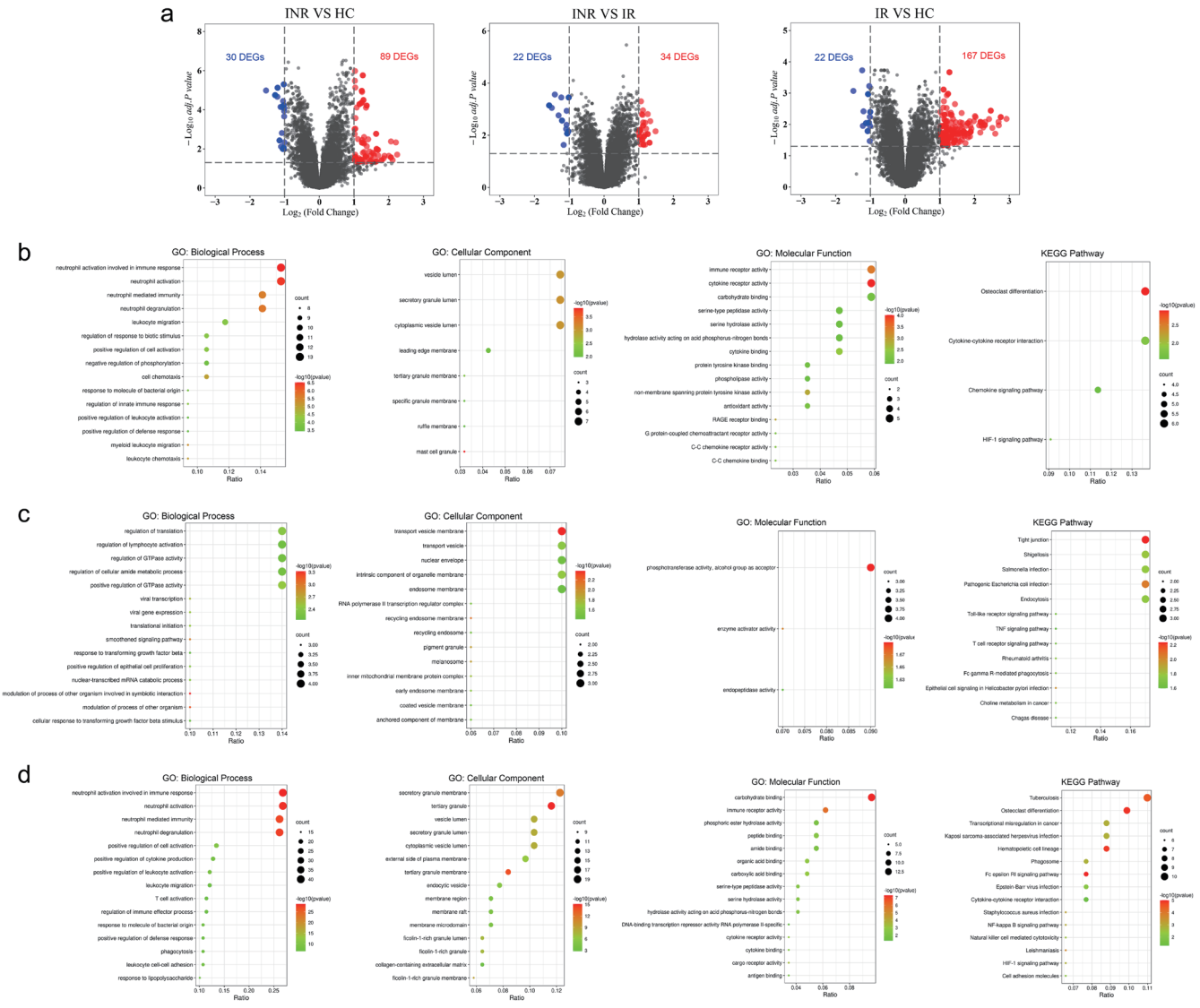

Fig. 1. Volcano plots and functional enrichment analyses of the upregulated and downregulated differentially expressed genes (DEGs). This figure presents the volcano plots for visualizing DEGs (a) and the functional enrichment analyses (b-d) for upregulated and downregulated DEGs in the immune non-responder (INR) group vs. healthy control (HC) group (b), INR group vs. immune responder (IR) group (c), and IR group vs. HC group (d). (a) Blue dots represent downregulated genes, and red dots represent upregulated genes. The x-axis represents the log2 fold change in gene expression, indicating the degree of upregulation (positive values) or downregulation (negative values). The y-axis represents the -log10 of the adjusted *P*-value, with higher values indicating greater statistical significance. (b-d) The x-axis shows the enriched terms (biological processes, cellular components, molecular functions, or pathways), and the y-axis represents the -log10 of the adjusted P-value, indicating the significance of enrichment. DEGs, differentially expressed genes; HC, healthy control; IR, immune responder; INR, immune non-responder.

DEGs were primarily related to phosphotransferase activity (alcohol group as acceptor), enzyme activator activity, and endopeptidase activity (Fig. 1c). KEGG pathway analysis demonstrated that the DEGs were mainly associated with tight junctions, endocytosis, rheumatoid arthritis, Fc gamma R-mediated phagocytosis, choline metabolism in cancer, Toll-like receptor signaling pathway, T cell receptor signaling pathway, and TNF signaling pathway (Fig. 1c).

In the IR vs. HC groups, GO analysis enriched 189 DEGs into 727 BP, 53 CC, and 78 MF terms (Fig. 1d). In the BP term, the DEGs were mainly involved in positive regulation of cell activation, positive regulation of cytokine production, positive regulation of leukocyte activation, leukocyte migration, regulation of immune effector processes, T cell activation, leukocyte cell-cell adhesion, response to bacterial molecules, phagocytosis, positive regulation of defense response, and response to lipopolysaccharide (Fig. 1d).In the CC term, the DEGs were mainly enriched in the secretory granule membrane, tertiary granule, secretory granule lumen, cytoplasmic vesicle lumen, vesicle lumen, external side of plasma membrane, tertiary granule membrane, endocytic vesicle, membrane raft, membrane microdomain, membrane region, ficolin-1-rich granule, ficolin-1-rich granule lumen, collagen-containing extracellular matrix, and ficolin-1-rich granule membrane (Fig. 1d). In the MF term, the DEGs were mainly related to carbohydrate binding, immune receptor activity, peptide binding, amide bind-

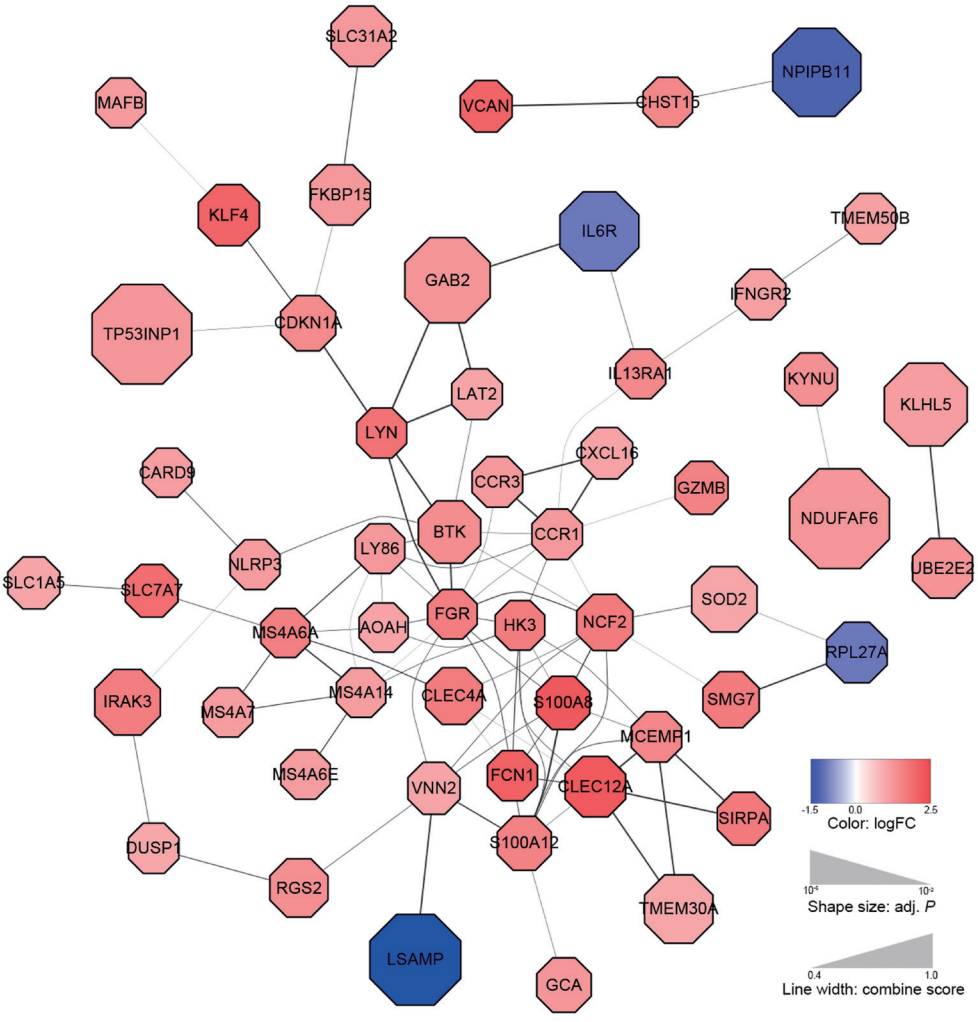

Fig. 2. The protein-protein interaction (PPI) network of differentially expressed genes (DEGs) in the immune non-responder (INR) group vs. healthy control (HC) group. Blue and red nodes represent the downregulated and upregulated DEGs, respectively. Edges indicate the interactions between the encoded proteins. DEGs, differentially expressed genes; HC, healthy control; INR, immune non-responder; PPI, protein-protein interaction.

ing, phosphoric ester hydrolase activity, carboxylic acid binding, organic acid binding, hydrolase activity acting on acid-phosphorus-nitrogen bonds, serine-type peptidase activity, serine hydrolase activity, DNA-binding transcription repressor activity (RNA polymerase II-specific), cargo receptor activity, cytokine receptor activity, cytokine binding, and antigen binding (Fig. 1d). KEGG pathway analysis revealed that the DEGs were mainly associated with hematopoietic cell lineage, transcriptional misregulation in cancer, Fc epsilon RI signaling pathway, phagosome, cytokine-cytokine receptor interaction, NF-kappa B signaling pathway, HIF-1 signaling pathway, and cell adhesion molecules (Fig. 1d).

Key candidate genes identification within DEGs' PPI network

To identify the key DEGs in the aforementioned groups, the PPI networks of the DEGs were constructed using the Search Tool for the Retrieval of Interacting Genes database and Cytoscape software. In the INR vs. HC groups, the PPI network of 119 identified DEGs contained 97 nodes and 92 edges, with the top ten highly connected genes being *FGR*, *CCR1*, *HK3*, *NCF2*, *S100A12*, *BTK*, *CLEC12A*, *S100A8*, *FCN1*, *LY86*, *MCEMP1*, *MS4A14*, *MS4A6A*, and *VNN2* (Fig. 2). In the INR vs. IR groups, the PPI network of 56 identified DEGs contained 35 nodes and 28 edges, with the top ten highly connected genes being *JUN*, *GLE1*, *HLA-C*, *SFRP1*, *TAF15*, *ACO1*, *CCL5*, *RPL9*, *ANXA8L1*, *ARPC1B*, *EXOSC6*, *HIPK2*, *HNRNPUL2*, *LRRN3*, *LSAMP*, *RAB35*, and *WASF3* (Fig. 3). In the IR vs. HC groups, the PPI network of 189 DEGs contained 154 nodes and 711 edges (Figs. 4 and S5).

Potential target proteins of DHA

To investigate the mechanism of DHA in the treatment of PLWH, the potential binding proteins of DHA were predicted using the STITCH online server and molecular docking. As indicated in Table S1 and Figure S6, the results from the STITCH database suggested that DHA might interact with 10 proteins, including TNFSF10B, UGT1A9, CYP3A4, CYP2C19, CASP3, CYP1A2, TP53, UGT1A7, UGT1A10, and UGT1A1.

As a natural product, DHA could potentially bind to more proteins. To explore this further, DHA was docked into all available protein crystal structures in the PDB database using the *Glide* module in the Schrodinger platform. The docking scores of proteins

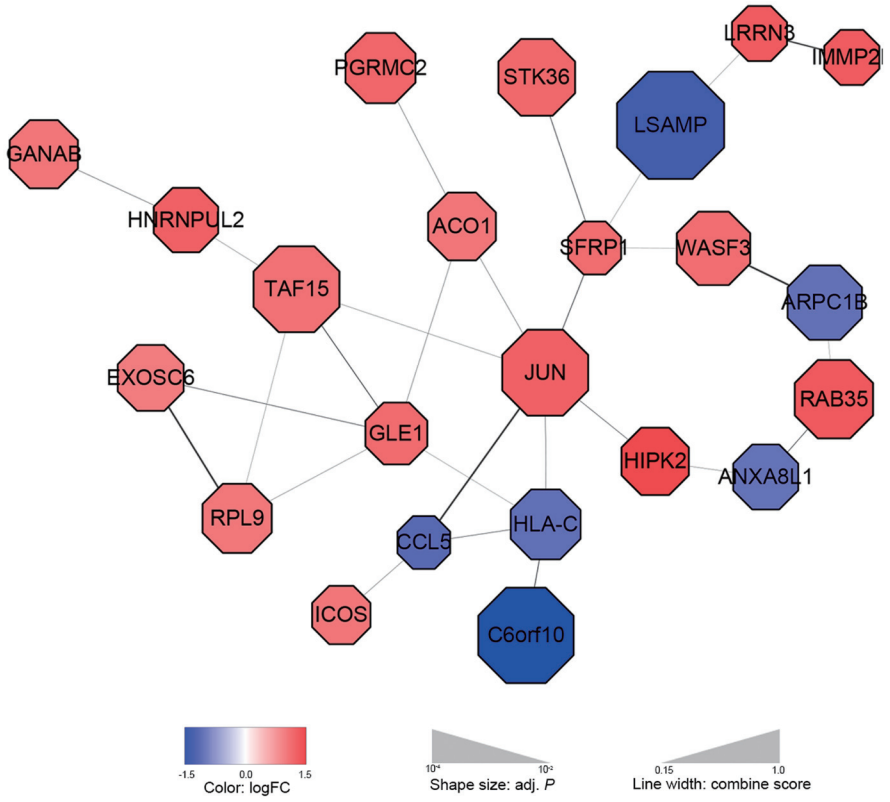

Fig. 3. The protein-protein interaction (PPI) network of differentially expressed genes (DEGs) in the immune non-responder (INR) group vs. immune responder (IR) group. Blue and red nodes represent the downregulated and upregulated DEGs, respectively. Edges indicate the interactions between the encoded proteins. DEGs, differentially expressed genes; IR, immune responder; INR, immune non-responder; PPI, protein-protein interaction.

with DHA below -7 kcal/mol were retained, resulting in the selection of 127 proteins (Table S2). Among the top-ranked 20 results (Table 1), six docking scores of the predicted target proteins with DHA were higher than those of natural ligands, including retinol-binding protein 2, odorant-binding protein (PDB ID: 1DZM), odorant-binding protein (PDB ID: 1HN2), retinaldehyde-binding protein 1, bile acid receptor, and pheromone-binding protein asp1. The bioactivities of these natural ligands with target proteins are generally in the nM and μM range, suggesting that DHA may have strong binding abilities to these target proteins.

HNMT encodes histamine *N*-methyltransferase, which was one of the DEGs between INRs and HCs. The docking score of DHA with HNMT was −9.42 kcal/mol, which is comparable to the natural ligand AdoHcy (−9.77 kcal/mol, experimental K_i = 6.9 μM).[35] This suggests that DHA may have a similar binding affinity to that of the original ligand AdoHcy. Further binding pattern analysis showed that DHA binds to the inhibitor pocket of HNMT (Fig. 5a and b), where DHA is embedded in hydrophobic pockets formed by Phe19, Phe22, Tyr146, Tyr147, Trp179, Trp183, and Phe243. The dioxo bridge structure of DHA also forms a hydrogen bond interaction with the phenolic hydroxyl group on the benzene ring of Tyr147's side chain (Fig. 5c and d). These results indicate that DHA might serve as an inhibitor of HNMT. Another DHA molecule docking target protein of interest, HIV-1 reverse transcriptase, is shown in Figure S7.

The ADMET properties of DHA

The ADMET properties of DHA were predicted using the ADMET predictive module of Pipeline Pilot (Version 8.5). As shown in Table 2, the water solubility of DHA was −4.39, indicating that DHA has low water solubility. The blood-brain barrier was −0.19, suggesting that DHA can pass through the blood-brain barrier to some extent. Cytochrome P450 2D6 binding (ADMET_EXT_CYP2D6) was −33.72, indicating that DHA might not bind to cytochrome P450 2D6. The human hepatotoxicity (ADMET_EXT_Hepatotoxic) was −3.88, suggesting that DHA may have hepatotoxic effects. The ADMET absorption level was 0, indicating good intestinal absorption. Plasma protein binding (ADMET_EXT_PPB) was −14.257, suggesting weak or no binding to plasma proteins. ADMET_AlogP98 and ADMET_PSA_2D were both within Lipinski's rule of five.

Flow cytometry detection

In this experiment, we treated PBMCs with different doses of DHA for 48 h and measured CD38 and HLA-DR expression on $CD4^+$ and $CD8^+$ T cells by flow cytometry (Fig. 6a). We found that the frequency of $CD38^-HLA\text{-}DR^+CD4^+$ T cells was significantly decreased after treatment with 1,000 μM DHA compared to the control (0 μM). However, no significant difference in the frequency of $CD38^+HLA\text{-}DR^+CD4^+$ T cells was observed at any DHA dose (Fig. 6b). Additionally, we observed that the frequency of $CD38^+HLA\text{-}DR^+CD8^+$ T cells was significantly decreased after treatment with 1,000 μM and 500 μM DHA compared to the control. However, although the frequency of $CD38^-HLA\text{-}DR^+CD8^+$ T cells gradually decreased after DHA treatment, no significant difference was observed (Fig. 6c). Furthermore, we did not ob-

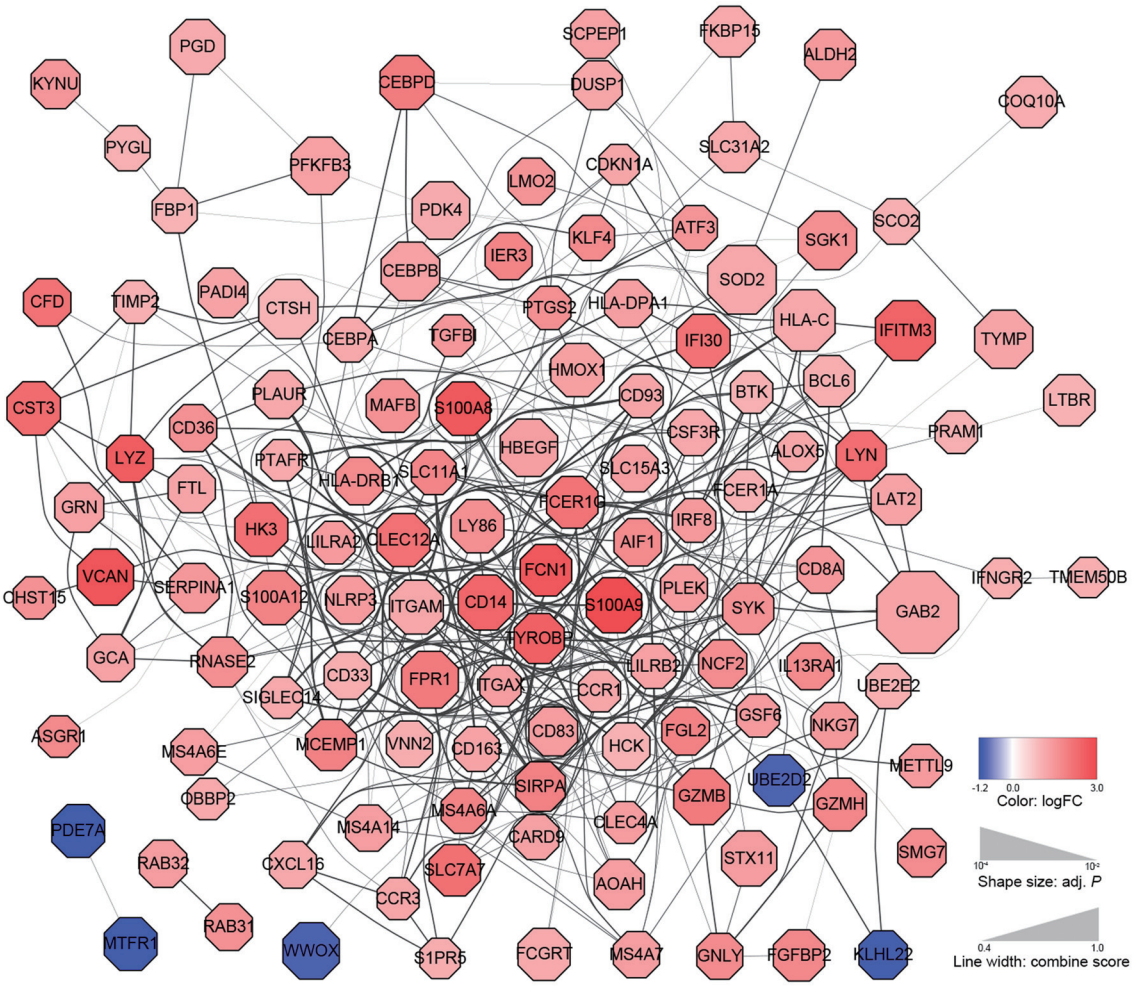

Fig. 4. The protein-protein interaction (PPI) network of differentially expressed genes (DEGs) in the immune responder (IR) group vs. healthy control (HC) group. Blue and red nodes represent the downregulated and upregulated DEGs, respectively. Edges indicate the interactions between the encoded proteins. Abbreviations: PPI: protein-protein interaction; DEGs: differentially expressed genes; IR: immune responder; HC: healthy control.

serve any significant changes in $CD38^{+}HLA\text{-}DR^{-}CD4^{+}$ T cells or $CD38^{+}HLA\text{-}DR^{-}CD8^{+}$ T cells before and after DHA treatment (data not shown). Additionally, we found that DHA inhibited T cell proliferation *in vitro* in INRs (Fig. S8)

Discussion

Incomplete immune reconstitution is characterized by chronic immune activation and systemic inflammation. However, the underlying physiological molecular mechanisms remain unclear. This study identified common significant potential mechanisms and pharmacological intervention strategies from seven independent studies (DEG analysis, enrichment analysis including GO and KEGG pathway analysis, PPI networks analysis, chemical association networks, molecular docking, ADMET, and flow cytometry detection).

Based on GO and KEGG enrichment analyses of the DEGs between INRs and HCs or IRs, "positive regulation of leukocyte activation", "leukocyte chemotaxis", and "regulation of lymphocyte activation" showed significant enrichment in the "biological process" category. In the "molecular function" category, the significantly affected molecular functions included "cytokine receptor activity", "immune receptor activity", "cytokine binding", "C-C chemokine receptor activity", and "C-C chemokine binding". The role of cytokines in HIV infection and T lymphocyte activation is complex and depends on various factors, including the stage of HIV infection, ART effects, and immune reconstitution.[36–38] For the KEGG pathway analysis, the canonical pathways associated with common DEGs are related to "cytokine-cytokine receptor interaction", "chemokine signaling pathway", and "T cell receptor signaling pathway". Interestingly, the DEGs are involved in the upregulation of known T lymphocyte activation pathways and incomplete immune reconstitution,[5,39–43] such as the "Toll-like receptor signaling pathway", "HIF-1 signaling pathway" and "TNF signaling pathway".

The RNA sequencing analysis aimed to uncover the molecular mechanisms of immune activation and inflammation in INRs compared to HC and IR groups. By focusing on DEGs from the NR vs. HC and INR vs. IR comparisons, we identified key pathways such as "cytokine-cytokine receptor interaction" and "T cell receptor signaling" that are relevant to immune dysregulation. These insights not only shed light on the potential therapeutic effects of

Table 1. Docking results of DHA with target proteins (top-ranked 20 *results)*

Predicted proteins	PDB ID	Bioactivities of natural ligands	Docking score (kcal/mol)	
			Natural ligands	DHA
HIV-1 reverse transcriptase	3M8P	IC_{50} = 2.1 nM	−13.63	−9.86
Muscarinic acetylcholine receptor m2, redesigned apo	5YC8	Kd = 6.4 nM	−13.75	−9.75
Retinol-binding protein 2	4GKC	Kd = 150 nM	−8.47	−9.71
Odorant-binding protein	1DZM	IC_{50} = 3.9 uM	−8.42	−9.61
HTH-type transcriptional repressor kstr	5CW8	Kd = 60 nM	−12.67	−9.60
Estrogen receptor	2FAI	Ki = 570 nM	−9.66	−9.51
Odorant-binding protei*n*	*1*HN2	Kd = 1.0 uM	−8.88	−9.50
Orphan nuclear receptor PXR	2O9I	IC_{50} = 40 nM	−11.12	−9.50
Antibody fab fragment mor03268 heavy chain	2JB6	Kd = 11 pM	−15.52	−9.45
Histamine n-methyltransferase	1JQD	Ki = 6.9 uM	−9.77	−9.42
Oxysterols receptor LXR-al*pha*	*3IPU*	*Ki* = 48 nM	−13.46	−9.36
Retinaldehyde-binding protein 1	4CIZ	Kd ⍰ 51 nM	−7.22	−9.32
Beta-glucosidase	1E55	Ki = 76 uM	−9.81	−9.28
Vitamin D3 receptor A	6FOB	IC_{50} = 23.5 nM	−12.13	−9.26
Estrogen receptor beta	2Z4B	Ki = 0.44 nM	−10.89	−9.24
Bile acid receptor	5Q11	IC_{50} = *7*.19 uM	−8.68	−9.24
Envelope glycoprotein gp160	5U7O	Kd = 73 nM	−13.12	−9.18
Mineralocorticoid receptor	5L7G	Ki = 16 nM	−11.90	−9.17
Vitamin D3 receptor	3VTB	IC_{50} = 0.5 nM	−14.45	−9.16
Pheromone-binding *protein* asp1	3D78	Kd = 23 nM	−7.84	−9.14

This table presents the top 20 target proteins predicted through docking analysis with DHA. The docking scores (in kcal/mol) reflect the binding affinity of DHA and the natural ligands to the respective target proteins. Lower docking scores indicate stronger binding affinities. The bioactivities of the natural ligands, such as IC50 (half-maximal inhibitory concentration), Kd (dissociation constant), and Ki (inhibition constant), are also listed for comparison. Abbreviations: PDB, Protein Data Bank; IC_{50}, half-maximal inhibitory concentration; K_d, dissociation constant; K_i, inhibition constant.

DHA but also suggest that further exploration of these pathways could help develop new treatments for patients with poor immune recovery on ART.

PPI network analysis provides detailed interactions among the DEGs. Compared with the DEGs of HCs or IRs, *FGR*, *CCR1*, *S100A12*, *CLEC12A*, *S100A8*, *LY86*, *MCEMP1*, and *CCL5* were the top highly interacted/connected genes in INRs. S100A8 and S100A12, collectively known as myeloid-related proteins, are calcium- and zinc-binding proteins that play a prominent role in regulating inflammatory processes and immune responses. High levels of these myeloid-related proteins in the serum of HIV-1-infected patients correlate with disease progression and low $CD4^+$ T-cell counts.[44] CCL5, a chemoattractant for memory T-helper cells and eosinophils, causes the release of histamine from basophils, activates eosinophils, and binds to several chemokine receptors, including CCR1, CCR3, CCR4, and CCR5.[45] CCL5 has been associated with resistance to HIV infection,[46] delayed AIDS progression,[45] and immune recovery status.[40] Interestingly, other DEGs in the PPI network also contribute to immune response regulation. Their proinflammatory activity involves the recruitment of leukocytes, promotion of cytokine and chemokine production, and regulation of leukocyte adhesion and migration. Further studies are warranted to elucidate the role of muscle-related genes in T lymphocyte activation in INRs. The PPI analysis also revealed key proteins, such as HNMT, which may play an important role in the immune dysregulation observed in INRs. While the PPI network provides insights into potential interactions between these proteins, further investigation into the extent of protein alterations at both RNA and protein levels is needed. This will allow us to better understand the functional impact of these interactions in the context of incomplete immune reconstitution.

So, how can we suppress inflammation and abnormal immune activation to recover $CD4^+$ T-cell counts? Much has been learned about potential treatments for incomplete immune reconstitution over the 30 years since the use of prednisone in HIV.[9] However, our recent review indicated that the majority of current candidates may not be ideal treatments for increasing $CD4^+$ T-cell counts in PLWH.[15] The immunological benefits and adverse events depend on factors such as safety, dosage, duration of use, and whether the treatment is combined with ART. Therefore, we have proposed the "SCAL" principles—safe, combined, adequate, and long—for $CD4^+$ T-cell recovery in PLWH and INRs.[15] Clearly, other safe, efficient, convenient, and affordable treatments are needed to stimulate this process. DHA possesses a broad range of bioactivities, including anti-inflammatory, immunosuppressive, and anti-tumor properties.[16,47] Protein docking results from our study indicated that DHA exerts anti-inflammatory effects via multiple potential target proteins, such as HNMT and HIV-1 reverse transcriptase.

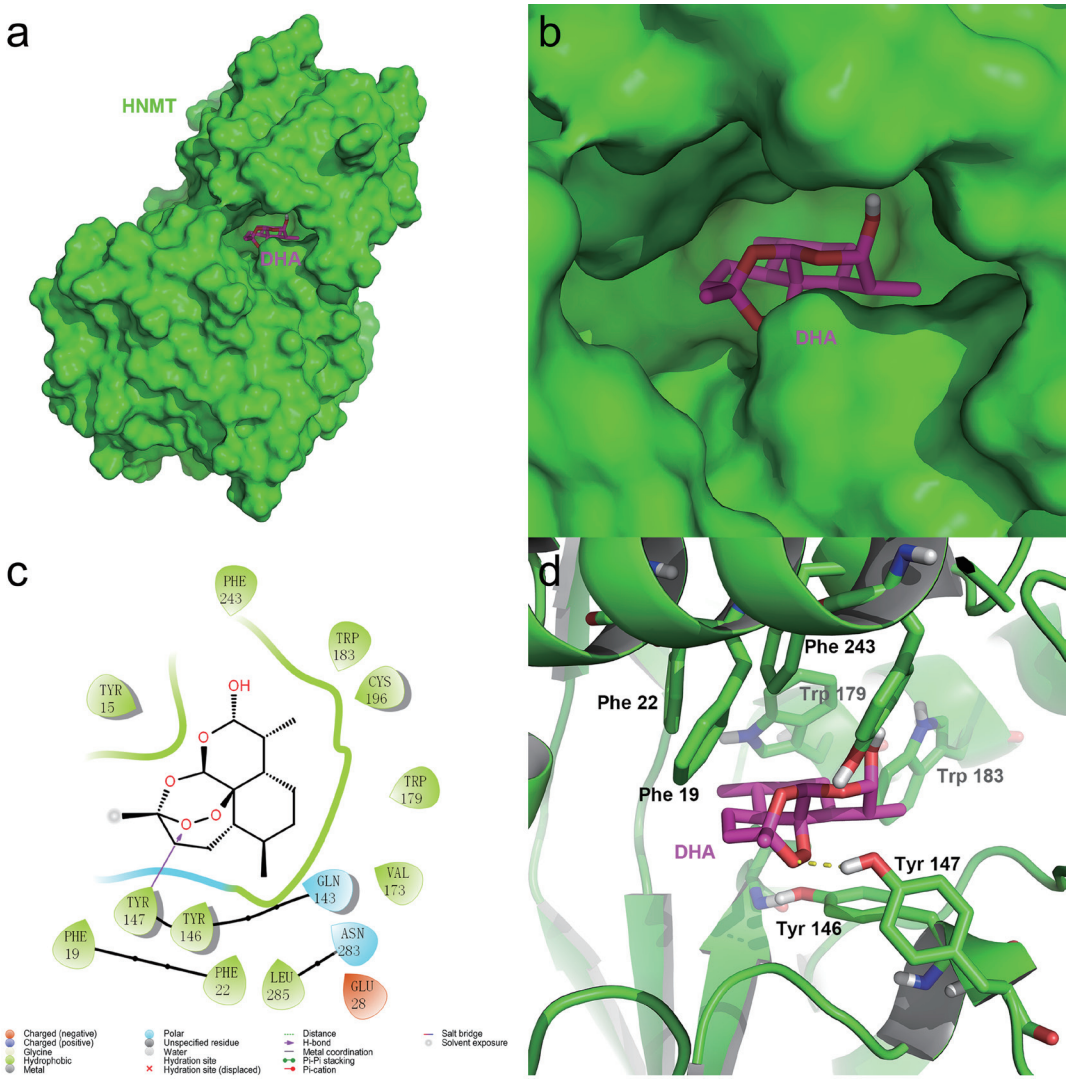

Fig. 5. Docking results between dihydroartemisinin (DHA) and histamine N-methyltransferase (HNMT). (a) Global docking diagram, showing DHA bound to the HNMT protein structure. (b) Detailed diagram showing the binding pocket of HNMT where DHA interacts. (c) Two-dimensional interaction diagram showing hydrogen bonds and hydrophobic interactions between DHA and HNMT. (d) Binding pattern diagram, highlighting the specific amino acids involved in the DHA-HNMT interaction. Abbreviations: DHA: dihydroartemisinin; HNMT: histamine N-methyltransferase.

Crucially, we found that the expression of immune activation markers on $CD4^+$ and $CD8^+$ T cells was significantly decreased after treatment with DHA compared to the control.

We are particularly interested in *HNMT*, which was one of the DEGs between INRs and HCs. DHA molecular docking in our study indicates that HNMT might be a potential therapeutic target in INRs. HNMT is responsible for histamine degradation, a biogenic amine involved in inflammation.[48,49] Previous studies have shown that gp120 of HIV is a powerful stimulus for the release of histamine and cytokines from basophils.[50] The histamine release caused by HIV might be involved in the development of HIV infection.[51] Interestingly, single nucleotide polymorphisms of *HNMT* are associated with the risk of common inflammatory and immune activation diseases, such as allergic asthma,[52–55] chronic urticaria,[56,57] and atopic dermatitis.[58] Moreover, artesunate, which is metabolized to DHA *in vivo*, possesses anti-allergic activity by blocking IgE-induced mast cell degranulation and histamine release.[59,60] Given that DHA might reduce histamine levels by regulating HNMT, thereby exerting anti-inflammatory effects, we speculate that HNMT may be another potential target of DHA for treating INRs. The docking results suggest that DHA may interact with HNMT and other proteins involved in immune regulation. Future studies will focus on how DHA treatment influences signaling pathways downstream of HNMT, with particular emphasis on immune-related pathways. Understanding these molecular effects will provide deeper insights into the therapeutic potential of DHA for immune non-responders.

On the other hand, interestingly, the antiviral activity of DHA against HIV-1 has not been reported. In this paper, we predict a new class of potent anti-HIV agents, indicating that DHA might inhibit HIV-1 replication by exerting anti-HIV-1 reverse transcriptase activity for the first time. The virally encoded gag protein is essential for efficient reverse transcription and plays a central role in sustaining viral replication. Moreover, considering that

Table 2. The predicted ADMET properties of DHA

ADMET properties	DHA
ADMET_Solubility/LogSw (mol/L)	−4.39
ADMET_Solubility_Level	2 (Low)
ADMET_BBB/LogBBB	−0.19
ADMET_BBB_Level	2 (Medium)
ADMET_EXT_CYP2D6	−33.72
ADMET_EXT_CYP2D6#Prediction	FALSE (a non-inhibitor)
ADMET_EXT_Hepatotoxic	−3.88
ADMET_EXT_Hepatotoxic#Prediction	TRUE (toxic)
ADMET_Absorption_Level	0 (Good)
ADMET_EXT_PPB	−14.257
ADMET_EXT_PPB#Prediction	FALSE (weak or non-binder)
ADMET_AlogP98	2.762
ADMET_PSA_2D	56.535

This table summarizes the predicted ADMET properties of DHA, including solubility, blood-brain barrier (BBB) permeability, cytochrome P450 2D6 (CYP2D6) binding, hepatotoxicity, plasma-protein binding (PPB), and other relevant pharmacokinetic parameters. The predictions are categorized into levels or binary outcomes (e.g., inhibitor or non-inhibitor, toxic or non-toxic), providing insights into DHA's pharmacokinetic and toxicological profiles. Abbreviations: ADMET, A - absorption, D - distribution, M - metabolism, E - excretion, T - toxicity; DHA, dihydroartemisinin; BBB, blood-brain barrier; CYP2D6, cytochrome P450 2D6 binding; PPB, plasma-protein binding; AlogP98, lipid-water distribution coefficient; PSA2D, polar surface area.

long-term low-level HIV-1 replication is one reason for poor immune reconstitution,[4–6] DHA is also expected to promote $CD4^+$ T-cell count recovery by inhibiting virus production from chronically and latently infected cells. Therefore, the clinical potential of DHA, targeting both anti-HIV-1 reverse transcription and anti-inflammatory mechanisms, is an attractive approach due to the safety and effectiveness of DHA. Furthermore, the ADMET properties of DHA indicate that it has good pharmacokinetic properties, druggability, and potential clinical application value.

Though DHA shows great potential, there are some limitations. GSE106792 data was generated with sort-purified $CD4^+$ memory T cells rather than PBMCs. In our study, we used PBMC samples, which include several types of cells, and this may impact the effects of DHA. Moreover, the gene expression profiles were from retrospective cohorts, and therefore, these findings must be prospectively validated in future studies. We confirmed that DHA could reduce T cell activation *in vitro*, but the complexity of incomplete immune reconstitution demands a more comprehensive analysis of clinical trials. Further studies should be conducted to determine whether DHA also provides therapeutic benefits in anti-HIV-1 treatment and promotes $CD4^+$ T-cell count recovery.

While our study examined DHA's effects on T cell activation and proliferation in INRs, it's important to assess whether similar effects occur in healthy controls. This would clarify whether DHA's actions are specific to the immune dysregulation in INRs. Future studies will address this to further validate our conclusions. Although we focused on HNMT based on the INR vs. HC RNA data and its position in the PPI network, we acknowledge the importance of investigating protein expression levels in actual patient samples. Differences in RNA expression do not always directly correlate with protein levels, which are often more functionally relevant. Future studies will aim to explore the expression of HNMT at the protein level to validate its role in immune non-responders, providing a more comprehensive understanding of its potential as a therapeutic target. While our study focuses on the immune-modulatory effects of DHA, we recognize the importance of thoroughly evaluating its safety profile. In future experiments, we plan to perform Annexin-V assays to assess cytotoxicity at each concentration of DHA. This will provide more robust evidence that DHA is non-toxic to cells at the concentrations used, further supporting its potential as a safe therapeutic option for immune non-responders. We recognize that PMA activates a broad range of cells, which may not fully reflect natural T cell activation. In future studies, we will use anti-CD3/anti-CD28 stimulation to more accurately mimic TCR engagement and assess activation markers like CD69 on $CD4^+$ and $CD8^+$ T cells.

Future directions

Further research is required to confirm the therapeutic potential of DHA in clinical settings, particularly its role in reducing immune activation and supporting $CD4^+$ T-cell recovery in INRs. Investigations into the molecular mechanisms underlying DHA's effects, including its interaction with HNMT and other immune-regulatory proteins, could provide additional insights. Clinical trials should focus on evaluating the safety, efficacy, and optimal dosing regimens of DHA, while also exploring its potential use in combination with existing ART regimes. Expanding these studies to include diverse patient populations and additional inflammatory conditions may further establish DHA's broader clinical relevance and utility.

Conclusions

Through functional analysis of the GEO database, we extracted a list of genes related to incomplete immune reconstitution and predicted that DHA may exert anti-inflammatory effects and promote $CD4^+$ T-cell count recovery via multiple potential target proteins. Moreover, our *in vitro* results demonstrate that the convenient, safe, and affordable DHA can reduce inflammation and T cell acti-

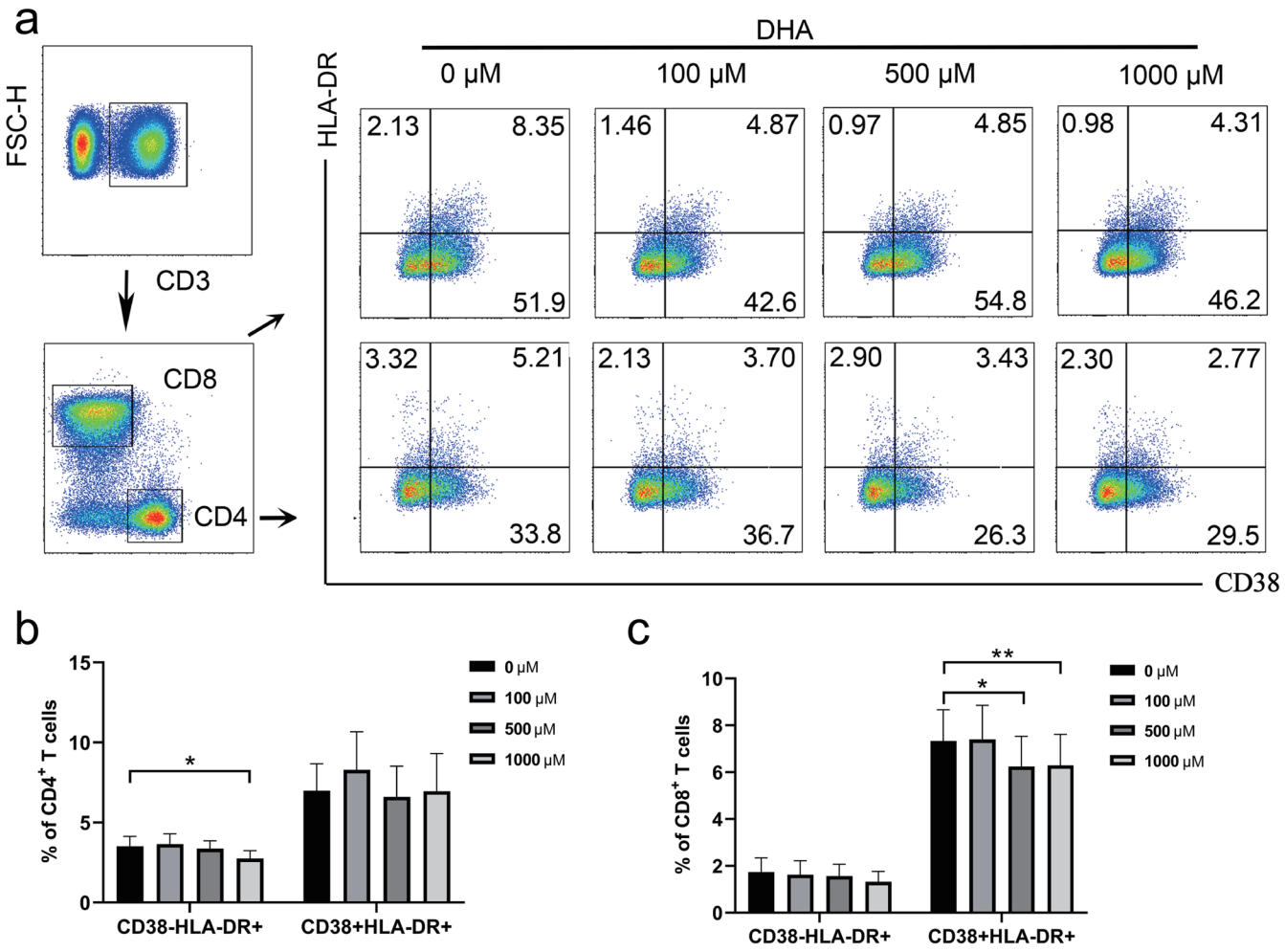

Fig. 6. Flow cytometry analysis of T cell activation in peripheral blood mononuclear cells (PBMCs) after dihydroartemisinin (DHA) treatment. (a) Flow diagram of T cell activation in PBMCs after treatment with various concentrations of DHA (1,000 μM, 500 μM, 100 μM). Freshly separated PBMCs were seeded at 1 × 10⍰6 cells/mL, stimulated with phytohemagglutinin (PHA, 5 μg/mL), and treated with/without DHA for 48 hours. Cells were gated on $CD3^+$ T cells, and CD38 and HLA-DR expression on $CD4^+$ and $CD8^+$ T cells were analyzed. (b) The frequencies of $CD38^-$ $HLA\text{-}DR^+$ $CD4^+$ T cells treated with different concentrations of DHA (0 μM, 100 μM, 500 μM, 1,000 μM). (c) The frequencies of $CD38^+$ $HLA\text{-}DR^+$ $CD8^+$ T cells treated with different concentrations of DHA (0 μM, 100 μM, 500 μM, 1,000 μM). *$P < 0.05$; **$P < 0.01$. Abbreviations: PBMCs: peripheral blood mononuclear cells; DHA: dihydroartemisinin; PHA: phytohemagglutinin.

vation in INRs. DHA may serve as a starting point for developing novel therapeutic approaches for incomplete immune reconstitution or as a primary research tool. Our findings provide additional data to help decode the complex interactions between DHA and incomplete immune reconstitution. Finally, further investigation of these genes and DHA could yield novel insights into the potential association between incomplete immune reconstitution and prognosis in a comprehensive manner.

Acknowledgments

None.

Funding

This work was supported by Beijing Research Ward Excellence Program (BRWEP2024W042180103 to Y.Z.), the Beijing Natural Science Foundation (7222091 to Y.Z.), the National Natural Science Foundation of China (82072271 to T.Z., 82241072 to T.Z., 82072294 to Z.L.), the High-level Public Health Technical Personnel Construction Project (2022-1-007 to T.Z.), and the Beijing Key Laboratory for HIV/AIDS Research (BZ0089 to T.Z.), the High-level Public Health Specialized Talents Project of Beijing Municipal Health commission(2022-02-20 to Z.L.), the Peak Talent Program of Beijing Hospital Authority (DFL20191701 to T.Z.), National Key Research and Development Program of China (2021YFC0122601), the Capital's Funds for Health Improvement and Research (2022-1-1151 to T.Z.), the Research and Translational Application of Clinical Characteristic Diagnostic and Treatment Techniques in Capital City (Z221100007422055 to T.Z.). Funding Support (2021037 to Y.Z.).

Conflict of interest

The authors have no conflict of interests related to this publication.

Author contributions

Study concept and design (YZ, JJ, ZL, TZ), acquisition, analysis, and interpretation of data (YZ, XD, RW, JJ, ZL), drafting the manuscript (YZ, XD, ZL), critical revision of the manuscript for important intellectual content (ZL, ZL, HW, TZ), obtained funding (YZ, ZL, HW, TZ), and study supervision (ZL, HW, TZ). All authors had full access to all of the data in the study. All authors are responsible for the integrity of data and the accuracy of data analysis and gave the publishing approval of this manuscript.

Ethical statement

Study materials were developed in accordance with the Declaration of Helsinki, along with ethical norms, guidelines, and HIV-related laws and regulations in China. The study was approved by the Ethics Committee of Beijing Youan Hospital, Capital Medical University (No. 2020147). All participants provided written informed consent.

Data sharing statement

The RNA sequencing data (GSE106792) used in support of the findings of this study have been deposited in the Gene Expression Omnibus repository (http://www.ncbi.nlm.nih.gov/geo/).

References

[1] Fauci AS, Lane HC. Four Decades of HIV/AIDS - Much Accomplished, Much to Do. N Engl J Med 2020;383(1):1–4. doi:10.1056/NEJMp1916753, PMID:32609976.

[2] Antiretroviral Therapy Cohort Collaboration. Life expectancy of individuals on combination antiretroviral therapy in high-income countries: a collaborative analysis of 14 cohort studies. Lancet 2008;372(9635):293–299. doi:10.1016/S0140-6736(08)61113-7, PMID:18657708.

[3] Deeks SG, Phillips AN. HIV infection, antiretroviral treatment, ageing, and non-AIDS related morbidity. BMJ 2009;338:a3172. doi:10.1136/bmj.a3172, PMID:19171560.

[4] Yang X, Su B, Zhang X, Liu Y, Wu H, Zhang T. Incomplete immune reconstitution in HIV/AIDS patients on antiretroviral therapy: Challenges of immunological non-responders. J Leukoc Biol 2020;107(4):597–612. doi:10.1002/JLB.4MR1019-189R, PMID:31965635.

[5] Deeks SG, Kitchen CM, Liu L, Guo H, Gascon R, Narváez AB, *et al*. Immune activation set point during early HIV infection predicts subsequent CD4+ T-cell changes independent of viral load. Blood 2004;104(4):942–947. doi:10.1182/blood-2003-09-3333, PMID:15117761.

[6] Kuller LH, Tracy R, Belloso W, De Wit S, Drummond F, Lane HC, *et al*. Inflammatory and coagulation biomarkers and mortality in patients with HIV infection. PLoS Med 2008;5(10):e203. doi:10.1371/journal.pmed.0050203, PMID:18942885.

[7] Premeaux TA, Moser CB, McKhann A, Hoenigl M, Laws EI, Aquino DL, *et al*. Plasma galectin-9 as a predictor of adverse non-AIDS events in persons with chronic HIV during suppressive antiretroviral therapy. AIDS 2021;35(15):2489–2495. doi:10.1097/QAD.0000000000003048, PMID:34366381.

[8] Vos AG, Dodd CN, Delemarre EM, Nierkens S, Serenata C, Grobbee DE, *et al*. Patterns of Immune Activation in HIV and Non HIV Subjects and Its Relation to Cardiovascular Disease Risk. Front Immunol 2021;12:647805. doi:10.3389/fimmu.2021.647805, PMID:34290695.

[9] McComsey GA, Whalen CC, Mawhorter SD, Asaad R, Valdez H, Patki AH, *et al*. Placebo-controlled trial of prednisone in advanced HIV-1 infection. AIDS 2001;15(3):321–327. doi:10.1097/00002030-200102160-00004, PMID:11273211.

[10] Piconi S, Parisotto S, Rizzardini G, Passerini S, Terzi R, Argenteri B, *et al*. Hydroxychloroquine drastically reduces immune activation in HIV-infected, antiretroviral therapy-treated immunologic nonresponders. Blood 2011;118(12):3263–3272. doi:10.1182/blood-2011-01-329060, PMID:21576701.

[11] Nakanjako D, Ssinabulya I, Nabatanzi R, Bayigga L, Kiragga A, Joloba M, *et al*. Atorvastatin reduces T-cell activation and exhaustion among HIV-infected cART-treated suboptimal immune responders in Uganda: a randomised crossover placebo-controlled trial. Trop Med Int Health 2015;20(3):380–390. doi:10.1111/tmi.12442, PMID:25441397.

[12] Hunt PW, Martin JN, Sinclair E, Epling L, Teague J, Jacobson MA, *et al*. Valganciclovir reduces T cell activation in HIV-infected individuals with incomplete CD4+ T cell recovery on antiretroviral therapy. J Infect Dis 2011;203(10):1474–1483. doi:10.1093/infdis/jir060, PMID:21502083.

[13] Tenorio AR, Chan ES, Bosch RJ, Macatangay BJ, Read SW, Yesmin S, *et al*. Rifaximin has a marginal impact on microbial translocation, T-cell activation and inflammation in HIV-positive immune non-responders to antiretroviral therapy - ACTG A5286. J Infect Dis 2015;211(5):780–790. doi:10.1093/infdis/jiu515, PMID:25214516.

[14] Hunt PW, Shulman NS, Hayes TL, Dahl V, Somsouk M, Funderburg NT, *et al*. The immunologic effects of maraviroc intensification in treated HIV-infected individuals with incomplete CD4+ T-cell recovery: a randomized trial. Blood 2013;121(23):4635–4646. doi:10.1182/blood-2012-06-436345, PMID:23589670.

[15] Zhang Y, Jiang T, Li A, Li Z, Hou J, Gao M, *et al*. Adjunct Therapy for CD4+ T-Cell Recovery, Inflammation and Immune Activation in People Living With HIV: A Systematic Review and Meta-Analysis. Front Immunol 2021;12:632119. doi:10.3389/fimmu.2021.632119, PMID:33679779.

[16] Wang J, Xu C, Liao FL, Jiang T, Krishna S, Tu Y. A Temporizing Solution to "Artemisinin Resistance". N Engl J Med 2019;380(22):2087–2089. doi:10.1056/NEJMp1901233, PMID:31018065.

[17] Huang X, Xie Z, Liu F, Han C, Zhang D, Wang D, *et al*. Dihydroartemisinin inhibits activation of the Toll-like receptor 4 signaling pathway and production of type I interferon in spleen cells from lupus-prone MRL/lpr mice. Int Immunopharmacol 2014;22(1):266–272. doi:10.1016/j.intimp.2014.07.001, PMID:25027631.

[18] Fan M, Li Y, Yao C, Liu X, Liu X, Liu J. Dihydroartemisinin derivative DC32 attenuates collagen-induced arthritis in mice by restoring the Treg/Th17 balance and inhibiting synovitis through down-regulation of IL-6. Int Immunopharmacol 2018;65:233–243. doi:10.1016/j.intimp.2018.10.015, PMID:30336338.

[19] Yan SC, Wang YJ, Li YJ, Cai WY, Weng XG, Li Q, *et al*. Dihydroartemisinin Regulates the Th/Treg Balance by Inducing Activated CD4+ T cell Apoptosis via Heme Oxygenase-1 Induction in Mouse Models of Inflammatory Bowel Disease. Molecules 2019;24(13):2475. doi:10.3390/molecules24132475, PMID:31284478.

[20] Zhang B, Liu P, Zhou Y, Chen Z, He Y, Mo M, *et al*. Dihydroartemisinin attenuates renal fibrosis through regulation of fibroblast proliferation and differentiation. Life Sci 2019;223:29–37. doi:10.1016/j.lfs.2019.03.020, PMID:30862567.

[21] Muhindo MK, Jagannathan P, Kakuru A, Opira B, Olwoch P, Okiring J, Nalugo N, Clark TD, Ruel T, Charlebois E, Feeney ME, Havlir DV, Dorsey G, Kamya MR. Intermittent preventive treatment with dihydroartemisinin-piperaquine and risk of malaria following cessation in young Ugandan children: a double-blind, randomised, controlled trial. Lancet Infect Dis 2019;19(9):962–972. doi:10.1016/S1473-3099(19)30299-3, PMID:31307883.

[22] Bangirana P, Conroy AL, Opoka RO, Semrud-Clikeman M, Jang JH, Apayi C, *et al*. Effect of Malaria and Malaria Chemoprevention Regimens in Pregnancy and Childhood on Neurodevelopmental and Behavioral Outcomes in Children at 12, 24, and 36 Months: A Randomized Clinical Trial. Clin Infect Dis 2023;76(4):600–608. doi:10.1093/cid/ciac815, PMID:36219705.

[23] Wallender E, Ali AM, Hughes E, Kakuru A, Jagannathan P, Muhindo MK, *et al*. Identifying an optimal dihydroartemisinin-piperaquine dosing regimen for malaria prevention in young Ugandan children. Nat Commun 2021;12(1):6714. doi:10.1038/s41467-021-27051-8, PMID:34795281.

[24] Younes SA, Talla A, Pereira Ribeiro S, Saidakova EV, Korolevskaya LB, Shmagel KV, *et al*. Cycling CD4+ T cells in HIV-infected immune nonresponders have mitochondrial dysfunction. J Clin Invest

2018;128(11):5083–5094. doi:10.1172/JCI120245, PMID:30320604.
[25] Ritchie ME, Phipson B, Wu D, Hu Y, Law CW, Shi W, *et al*. limma powers differential expression analyses for RNA-sequencing and microarray studies. Nucleic Acids Res 2015;43(7):e47. doi:10.1093/nar/gkv007, PMID:25605792.
[26] Yu G, Wang LG, Han Y, He QY. clusterProfiler: an R package for comparing biological themes among gene clusters. OMICS 2012;16(5):284–287. doi:10.1089/omi.2011.0118, PMID:22455463.
[27] Huang da W, Sherman BT, Lempicki RA. Systematic and integrative analysis of large gene lists using DAVID bioinformatics resources. Nat Protoc 2009;4(1):44–57. doi:10.1038/nprot.2008.211, PMID:19131956.
[28] Szklarczyk D, Gable AL, Lyon D, Junge A, Wyder S, Huerta-Cepas J, *et al*. STRING v11: protein-protein association networks with increased coverage, supporting functional discovery in genome-wide experimental datasets. Nucleic Acids Res 2019;47(D1):D607–D613. doi:10.1093/nar/gky1131, PMID:30476243.
[29] Shannon P, Markiel A, Ozier O, Baliga NS, Wang JT, Ramage D, *et al*. Cytoscape: a software environment for integrated models of biomolecular interaction networks. Genome Res 2003;13(11):2498–504. doi:10.1101/gr.1239303, PMID:14597658.
[30] Szklarczyk D, Santos A, von Mering C, Jensen LJ, Bork P, Kuhn M. STITCH 5: augmenting protein-chemical interaction networks with tissue and affinity data. Nucleic Acids Res 2016;44(D1):D380–D384. doi:10.1093/nar/gkv1277, PMID:26590256.
[31] Sillman B, Woldstad C, Mcmillan J, Gendelman HE. Neuropathogenesis of human immunodeficiency virus infection. Handb Clin Neurol 2018;152:21–40. doi:10.1016/B978-0-444-63849-6.00003-7, PMID:29604978.
[32] Maharshi S, Sharma BC, Srivastava S, Jindal A. Randomised controlled trial of lactulose versus rifaximin for prophylaxis of hepatic encephalopathy in patients with acute variceal bleed. Gut 2015;64(8):1341–1342. doi:10.1136/gutjnl-2014-308521, PMID:25320105.
[33] Friesner RA, Banks JL, Murphy RB, Halgren TA, Klicic JJ, Mainz DT, *et al*. Glide: a new approach for rapid, accurate docking and scoring. 1. Method and assessment of docking accuracy. J Med Chem 2004;47(7):1739–1749. doi:10.1021/jm0306430, PMID:15027865.
[34] Halgren TA, Murphy RB, Friesner RA, Beard HS, Frye LL, Pollard WT, *et al*. Glide: a new approach for rapid, accurate docking and scoring. 2. Enrichment factors in database screening. J Med Chem 2004;47(7):1750–1759. doi:10.1021/jm030644s, PMID:15027866.
[35] Horton JR, Sawada K, Nishibori M, Zhang X, Cheng X. Two polymorphic forms of human histamine methyltransferase: structural, thermal, and kinetic comparisons. Structure 2001;9(9):837–849. doi:10.1016/s0969-2126(01)00643-8, PMID:11566133.
[36] Rosignoli G, Cranage A, Burton C, Nelson M, Steel A, Gazzard B, *et al*. Expression of PD-L1, a marker of disease status, is not reduced by HAART in aviraemic patients. AIDS 2007;21(10):1379–1381. doi:10.1097/QAD.0b013e3281de7296, PMID:17545722.
[37] Burgess K, Price P, James IR, Stone SF, Keane NM, Lim AY, *et al*. Interferon-gamma responses to Candida recover slowly or remain low in immunodeficient HIV patients responding to ART. J Clin Immunol 2006;26(2):160–167. doi:10.1007/s10875-006-9008-4, PMID:16568352.
[38] Mercurio V, Fitzgerald W, Molodtsov I, Margolis L. Persistent Immune Activation in HIV-1-Infected Ex Vivo Model Tissues Subjected to Antiretroviral Therapy: Soluble and Extracellular Vesicle-Associated Cytokines. J Acquir Immune Defic Syndr 2020;84(1):45–53. doi:10.1097/QAI.0000000000002301, PMID:32032302.
[39] Paton NI, Goodall RL, Dunn DT, Franzen S, Collaco-Moraes Y, Gazzard BG, *et al*. Effects of hydroxychloroquine on immune activation and disease progression among HIV-infected patients not receiving antiretroviral therapy: a randomized controlled trial. JAMA 2012;308(4):353–361. doi:10.1001/jama.2012.6936, PMID:22820788.
[40] Yeregui E, Viladés C, Domingo P, Ceausu A, Pacheco YM, Veloso S, *et al*. High circulating SDF-1and MCP-1 levels and genetic variations in CXCL12, CCL2 and CCR5: Prognostic signature of immune recovery status in treated HIV-positive patients. EBioMedicine 2020;62:103077. doi:10.1016/j.ebiom.2020.103077, PMID:33166788.
[41] Arenzana-Seisdedos F, Parmentier M. Genetics of resistance to HIV infection: Role of co-receptors and co-receptor ligands. Semin Immunol 2006;18(6):387–403. doi:10.1016/j.smim.2006.07.007, PMID:16978874.
[42] Andrade-Santos JL, Carvalho-Silva WHV, Coelho AVC, Souto FO, Crovella S, Brandão LAC, *et al*. IL18 gene polymorphism and its influence on CD4+ T-cell recovery in HIV-positive patients receiving antiretroviral therapy. Infect Genet Evol 2019;75:103997. doi:10.1016/j.meegid.2019.103997, PMID:31401307.
[43] Espineira S, Flores-Piñas M, Chafino S, Viladés C, Negredo E, Fernández-Arroyo S, *et al*. Multi-omics in HIV: searching insights to understand immunological non-response in PLHIV. Front Immunol 2023;14:1228795. doi:10.3389/fimmu.2023.1228795, PMID:37649488.
[44] Ryckman C, Robichaud GA, Roy J, Cantin R, Tremblay MJ, Tessier PA. HIV-1 transcription and virus production are both accentuated by the proinflammatory myeloid-related proteins in human CD4+ T lymphocytes. J Immunol 2002;169(6):3307–3313. doi:10.4049/jimmunol.169.6.3307, PMID:12218151.
[45] Flórez-Álvarez L, Hernandez JC, Zapata W. NK Cells in HIV-1 Infection: From Basic Science to Vaccine Strategies. Front Immunol 2018;9:2290. doi:10.3389/fimmu.2018.02290, PMID:30386329.
[46] Silva MJA, Marinho RL, Dos Santos PAS, Dos Santos CS, Ribeiro LR, Rodrigues YC, *et al*. The Association between CCL5/RANTES SNPs and Susceptibility to HIV-1 Infection: A Meta-Analysis. Viruses 2023;15(9):1958. doi:10.3390/v15091958, PMID:37766364.
[47] Zhang T, Zhang Y, Jiang N, Zhao X, Sang X, Yang N, *et al*. Dihydroartemisinin regulates the immune system by promotion of CD8+ T lymphocytes and suppression of B cell responses. Sci China Life Sci 2020;63(5):737–749. doi:10.1007/s11427-019-9550-4, PMID:31290095.
[48] Hon YY, Jusko WJ, Zhou HH, Chen GL, Guo D, Zhou G, *et al*. Endogenous histamine and cortisol levels in subjects with different histamine N-methyltransferase C314T genotypes: a pilot study. Mol Diagn Ther 2006;10(2):109–114. doi:10.1007/BF03256450, PMID:16669609.
[49] Maintz L, Novak N. Histamine and histamine intolerance. Am J Clin Nutr 2007;85(5):1185–1196. doi:10.1093/ajcn/85.5.1185, PMID:17490952.
[50] Rossi FW, Prevete N, Rivellese F, Lobasso A, Napolitano F, Granata F, *et al*. HIV-1 Nef promotes migration and chemokine synthesis of human basophils and mast cells through the interaction with CXCR4. Clin Mol Allergy 2016;14:15. doi:10.1186/s12948-016-0052-1, PMID:27822141.
[51] Pedersen M, Nielsen CM, Permin H. HIV antigen-induced release of histamine from basophils from HIV infected patients. Mechanism and relation to disease progression and immunodeficiency. Allergy 1991;46(3):206–212. doi:10.1111/j.1398-9995.1991.tb00572.x, PMID:1711797.
[52] Szczepankiewicz A, Bręborowicz A, Sobkowiak P, Popiel A. Polymorphisms of two histamine-metabolizing enzymes genes and childhood allergic asthma: a case control study. Clin Mol Allergy 2010;8:14. doi:10.1186/1476-7961-8-14, PMID:21040557.
[53] Jones BL, Sherwin CM, Liu X, Dai H, Vyhlidal CA. Genetic Variation in the Histamine Production, Response, and Degradation Pathway Is Associated with Histamine Pharmacodynamic Response in Children with Asthma. Front Pharmacol 2016;7:524. doi:10.3389/fphar.2016.00524, PMID:28101058.
[54] Anvari S, Vyhlidal CA, Dai H, Jones BL. Genetic Variation along the Histamine Pathway in Children with Allergic versus Nonallergic Asthma. Am J Respir Cell Mol Biol 2015;53(6):802–809. doi:10.1165/rcmb.2014-0493OC, PMID:25909280.
[55] Raje N, Vyhlidal CA, Dai H, Jones BL. Genetic variation within the histamine pathway among patients with asthma—a pilot study. J Asthma 2015;52(4):353–362. doi:10.3109/02770903.2014.973501, PMID:25295384.
[56] Kim SH, Kang YM, Kim SH, Cho BY, Ye YM, Hur GY, *et al*. Histamine N-methyltransferase 939A>G polymorphism affects mRNA stability in patients with acetylsalicylic acid-intolerant chronic urticaria. Allergy 2009;64(2):213–221. doi:10.1111/j.1398-9995.2008.01795.x, PMID:19178400.
[57] Kolkhir P, Giménez-Arnau AM, Kulthanan K, Peter J, Metz M, Maurer M. Urticaria. Nat Rev Dis Primers 2022;8(1):61. doi:10.1038/s41572-022-00389-z, PMID:36109590.
[58] Kennedy MJ, Loehle JA, Griffin AR, Doll MA, Kearns GL, Sullivan JE, *et al*. Association of the histamine N-methyltransferase C314T

(Thr105Ile) polymorphism with atopic dermatitis in Caucasian children. Pharmacotherapy 2008;28(12):1495–1501. doi:10.1592/phco.28.12.1495, PMID:19025430.

[59] Cheng C, Ng DS, Chan TK, Guan SP, Ho WE, Koh AH, *et al*. Anti-allergic action of anti-malarial drug artesunate in experimental mast cell-mediated anaphylactic models. Allergy 2013;68(2):195–203. doi:10.1111/all.12077, PMID:23253152.

[60] Li R, Tong R, Zhang JL, Zhang Z, Deng M, Hou G. Comprehensive molecular analyses of cuproptosis-related genes with regard to prognosis, immune landscape, and response to immune checkpoint blockers in lung adenocarcinoma. J Cancer Res Clin Oncol 2024;150(5):246. doi:10.1007/s00432-024-05774-7, PMID:38722401.